Quantum Dot Light-Emitting Diode Based Photomedicine: In Vitro Results to Date and Tunable Features for Targeted Phototherapy

M Alejandro Triana[1,2,3], Hamid El Hamidi[4], Jonathan Celli[4], Raymond Lanzafame[5], Shin-Tson Wu[3], Yajie Dong[1,2,3,5]

ma424390@ucf.edu
[1]Nanoscience Technology Center, University of Central Florida, Orlando, FL, 32826, USA
[2]Department of Materials Science & Engineering, University of Central Florida, Orlando, FL, 32816, USA
[3]College of Optics and Photonics, University of Central Florida, Orlando, FL 32816, USA
[4]Department of Physics, University of Massachusetts Boston, Boston, MA, 02125, USA
[5]QLEDcures LLC, Orlando, FL, 32826, USA
Keywords: Quantum dot light-emitting diodes, photosensitizer, photodynamic therapy, photobiomodulation

ABSTRACT

Our recent in-vitro studies in photodynamic therapy and photobiomodulation have demonstrated the high potential of quantum dot light-emitting diodes (QLEDs) as alternative photomedical light sources. Herein, we summarize the QLED in-vitro results to date and present the tunable features making QLEDs unique for targeted phototherapy of disorders and conditions.

1 Introduction

Narrow emission bandwidth, high efficiency (EQE >20% with light outcoupling), high-power density, and low-cost solution processing, are all attractive features of quantum dot light-emitting diodes (QLEDs) for display, lighting, and emerging applications. Other promising features of QLEDs are the emission wavelength tunability, emitting area scalability, and multiple form factors, with the potential to broaden the application range and boost the earlier commercialization of QLEDs. Indeed, QLEDs have demonstrated highly desired features and satisfactory in-vitro results as light sources for emerging photomedical therapies, i.e., photodynamic therapy (PDT) and photobiomodulation (PBM). The efficacy and benefits of these phototherapies have already been clinically proven, however, important limitations of the mainstream photomedical light sources are preventing their widespread adoption. Among the main limitations, LED arrays have poor flexibility and inhomogeneous irradiance, while laser systems are bulky and expensive.

Previously, our group has proposed low-cost solution-processed flexible QLEDs with desired form factors, narrow emission spectrum, and high-power density at clinically relevant deep red wavelengths in order to enable wider adoption of photomedicine across the healthcare system. Since 2017, we have worked on in-vitro testing of QLEDs and the development of QLEDs as ideal photomedical light sources. Herein we summarize and discuss in detail our QLED based in-vitro studies conducted to date. On the other hand, we add on the development of new QLEDs and provide a perspective in targeted phototherapy by exploiting tunable features of QLEDs such as emission wavelength, emitting area, and form factor.

2 In vitro test results

We have proved the capability of QLEDs as photomedical light sources by PDT and PBM in vitro testing and parallel comparison with the efficacy of commercial LEDs. Here we summarize reported in vitro results and present new results as well.

For the first PBM in vitro study [1,2], three cell lines were cultured: a human epithelial cell line (HEp-2 cells) and two fibroblast cell lines from mouse (L929 and 3T3). Irradiation of the culture wells was performed to deliver 4 J cm^{-2} in 10 min at ~8 mW cm^{-2}. At 24 h post-irradiation, cell metabolism was assessed by a common colorimetric assay (MTT). The QLED-based PBM treatment increased the cell metabolism for the three cell lines HEp-2, L929 and 3T3, by 27.9, 12.5 and 26.2% over the control systems, respectively. The cell metabolic enhancement is summarized in the bar chart of Figure 1a. Importantly, the results were comparable to those of the parallel LED in vitro experiment even though the peak wavelength of the QLED (620 nm) and LED (670 nm) devices differed.

Subsequently, we used QLEDs for in vitro test of PBM based wound healing using a 2D scratch model [3]. Cultures of HEp-2 and L929 cells with a confluent monolayer were scored to leave a scratch of approx. 0.4–0.5 mm in width. Then, photoirradiation was performed with a 626 nm QLED to deliver either 2 J cm^{-2} in 5 min or 4 J cm^{-2} in 10 min at ~ 8 mW cm^{-2}. A parallel experiment was carried out using a commercial 670 nm NASA LED, with the same light dosages and culture conditions. The best closure rate ratios (CRRs) at 24 h for the QLED treatment of the cell lines HEp-2 and L929 were achieved at 4 J cm^{-2} in 10 min, 64% and 263% with respect to the control (see Figures 1b and 1c). In addition, mildly higher CRRs were observed for LEDs at the same

fluence. This discrepancy was attributed to the difference in peak wavelength for irradiation, since longer deep red wavelengths are known to be more effective in promoting wound healing.

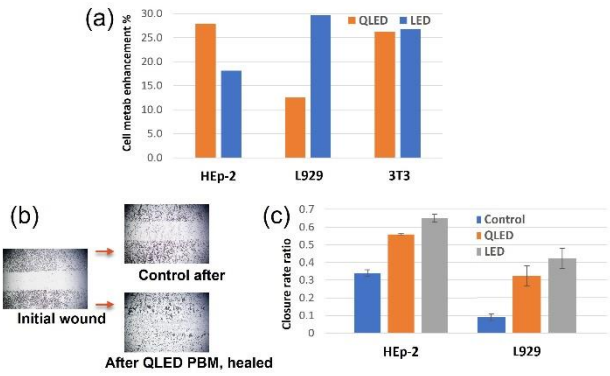

Fig 1. *QLED based in-vitro PBM testing.* a) Cell metabolism enhancement of cells lines HEp-2, L929, and 3T3 after irradiation with either QLED or LED, and respect to control cultures. b) Cell migration test based on a "2D scratch model". c) CRR of cell lines HEp-2 and L929, 24 h after irradiation with QLED, LED, and without irradiation (control systems).

For the first PDT in vitro test [2], 3D cultures of A431 cells were photosensitized by administration of ALA, leading to accumulation of PpIX prior to light activation. A431 cells are a human cell line from an epidermoid carcinoma in the skin. We compared control cells with no light treatment, cells with LED-based PDT, and cells with QLED-based PDT. In order to deliver the same total light dose of 30 J cm^{-2}, irradiation with the QLED and LED lasted 4.75 h (~1.8 mW cm^{-2}) and 4 min (~130 mW cm^{-2}), respectively. The 3D cultures were labeled using fluorescent vital dye 24 h after PDT treatment, calcein labeled live cells green, while ethidium bromide labeled dead cells red. Both QLED and LED sources achieved photo-destruction of 3D tumor nodules. Importantly, the quantitative image processing of multiple replicates revealed a slightly higher efficacy for QLED-based PDT considering the residual tumor viabilities, 0.61 ± 0.04 and 0.53 ± 0.08 for LEDs and QLEDs, respectively. The respective fluorescent culture images taken 24 h post-PDT treatment are shown in Figure 2a.

A new in vitro PDT test on TR146 cells is presented here. TR146 is a human squamous cell carcinoma whose primary tumor originated in the buccal mucosa. In this test a light dose of 66 J cm^{-2} was delivered over a period of 150 min using LED and QLED sources. According to the residual cell viabilities, 0.65 ± 0.03 and 0.52 ± 0.06 corresponding to LEDs and QLEDs, a higher efficacy of the QLEDs based in vitro PDT was once again observed over commercial LEDs. The better performance of QLEDs was attributed to better irradiation uniformity of the QLED-based PDT, as can be observed in the fluorescent culture images shown in Figure 2b.

The on-glass QLEDs used for the in vitro tests had pixels of 16 mm^2 each, as illustrated in Figure 2c. Typically, irradiation from only one pixel was sufficient for each of the in vitro tests. The evaluation of the QLEDs efficacy in antibacterial PDT (aPDT) was also conducted [4]. Methicillin resistant S. aureus (MRSA), an antibiotic-resistant bacterium, was treated with 10 uM Photofrin and 100 mM potassium iodide, and then illuminated with a QLED powered by a battery pack of two 3 V coin cells (shown in inset of figure 2d). Remarkably, the survival fraction of MRSA dropped to less than 10^{-6} after 1 h illumination, as observed in Figure 2d.

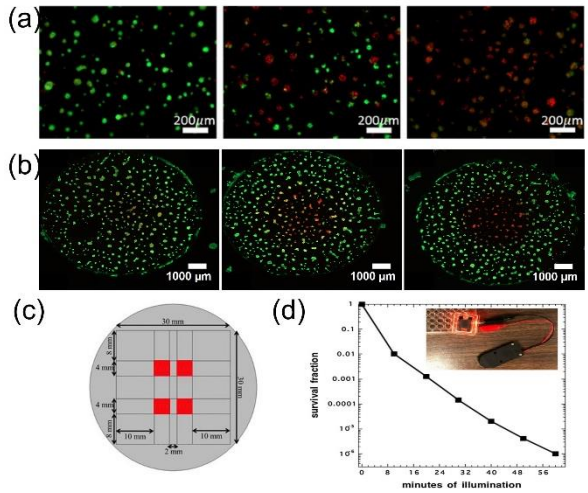

Fig 2. *QLED based in-vitro PDT testing.* Fluorescent vital-dye labeled 3D cultures 24 h post-PDT treatment corresponding to a) A431 and b) TR146 cells. Left: control cells without light treatment; Center: LED-based PDT; Right: QLED-based PDT. c) Pattern of the QLEDs with 16 mm^2 pixels used in the in vitro tests. d) Survival fraction evolution of MRSA under QLED-based PDT using Photofrin as PS.

3 QLED tunable features for targeted phototherapy

3.1 Emission wavelength tunability

We have precisely tuned the QLEDs emission to two wavelengths (630 and 650 nm) for the optimization of PDT and PBM treatments. Highly efficient QDs with different emission peaks (at 625 and 646 nm) and narrow emission spectra (FWHM < 30 nm) were obtained by tuning the QD synthesis conditions (QDs' size and composition). Subsequently, these QDs were used to fabricate QLEDs. According to the red-shift observed between the electroluminescence (EL) spectrum of QLEDs and the photoluminescence (PL) spectrum of the

QDs solution, the QLEDs obtained had emission wavelength around 630 and 650 nm, corresponding to a ~4-5 nm red-shift. These wavelengths were carefully selected to match the absorption of four specific photosensitizers (PSs) for targeted photomedicine as follows:

- Porfimer sodium (Photofrin ®, abs peak @ 630 nm), an FDA approved PS used for various PDT cancer treatments
- Protoporphyrin IX (PpIX, 4th Q band ~630 nm), an endogenous PS that accumulates after administration of aminolevulinic acid (ALA). This PS has been developed for a wide range of applications and it is FDA approved for PDT treatment of actinic keratosis
- Temoporfin (652 nm), a PS used for PDT treatment of squamous cell carcinoma of the head and neck
- Methylene Blue (MB, max. absorption peak ~655 nm), a PS used for antibacterial and antiviral PDT

QLEDs with EL peaks at ~630 nm match well with the absorption peaks of Photofrin and PpIX, while QLEDs with EL peak at ~650 nm can be used for excitation of Temoporfin and MB. Overlapping of the EL spectra of the QLEDs and absorption spectra of the PSs is shown in Figure 3a for Photofrin and PpIX, and Figure 3b for Temoporfin and MB. In addition to meeting these PDT needs, the 650 nm light was also shown to stimulate cytochrome C, the primary light absorbing chromophore for PBM.

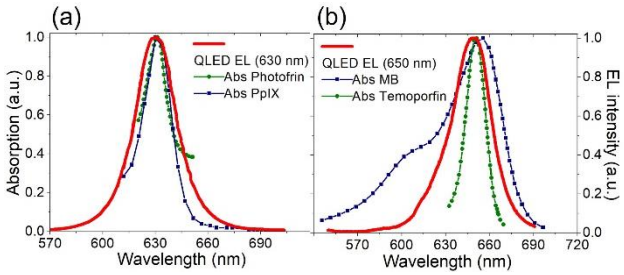

Fig 3. *Emission wavelength tunability*. a) overlapping of the absorption spectra of Photofrin and PpIX, and the EL spectrum of a 630 nm QLED; b) overlapping of the absorption spectra of Temoporfin and MB, and the EL spectrum of a 650 nm QLED.

3.2 Form factor and emitting area tunability

Flexible QLEDs are in obligatory demand for wearable light source systems, therefore, we have focused efforts to replace the rigid substrates and covers of our on-glass QLEDs for flexible plastic substrates and laminated barriers, while preserving the same functional stack of the QLEDs used for in vitro test to date. The best performing flexible red-emitting QLEDs we have achieved have the following inverted structure: ITO-PEN/ZnO:Cs2CO3/CdSe-ZnS-CdZnS QDs/Spiro-2NPB/HAT-CN/Al. Where, ITO-PEN is a commercial flexible conductive substrate made of indium tin oxide on polyethylene naphthalate, with a thickness of 125 µm, transmittance ≥ 80 %, and sheet resistance of 6-8 Ω/sq. A detailed description of the fabrication process can be found at Triana et al. 2020 [5]. For the encapsulation of the devices, a flexible getter was first laminated on top, and later, barrier films were laminated on the top and bottom of each device as depicted in Figure 4a. Because of the need for large-area QLEDs for the treatment of large lesions, our first flexible QLEDs achieved by this process had a pixel size of 8 mm^2, in contrast to small pixels used for display applications (≤ 1 mm^2). These flexible QLEDs exhibited a record brightness of 4.22×10^4 cd m^{-2} at 5.8 V, peak EQE of 8.3%, and low efficiency roll-off over the measured range. Remarkably, the optical power density (OPD) of ~71 mW cm^{-2}, estimated from the maximum brightness, largely surpassed the OPD requirement for application in low-irradiance PDT and PBM phototherapies (~2-10 mW cm^{-2}) [6]. The J-L-V curves of the flexible QLED with 8 mm^2 pixel are presented in Figure 4b.

Herein, we report on flexible ITO-PEN QLEDs with pixel size of 4 cm^2 (2x2 cm^2) achieved by the same fabrication process and inverted structure. The picture from Figure 4c shows a bent encapsulated QLED with an emitting area of 4 cm^2, powered with a battery pack of 3 V in air. This large-pixel QLED had the same substrate size (5x5 cm^2) and weight (1.4 g) as those of the QLEDs with 8 mm^2 pixels. The corresponding EL spectrum (see Figure 4d) had an emission peak centered at 627 nm and narrow FWHM of 29 nm. In order to evaluate the homogeneity of the illumination area in these large pixels, we measured the luminance at 9 different positions as indicated in the inset of Figure 4d. By eliminating the hot spot (1) near the electrical contact of the negative electrode, a relatively low standard deviation of 17.3% was obtained. In Figure 4e we provide the L-V curve and corresponding OPD-V curve of the 4 cm^2 QLEDs in a voltage range of 3 – 4.5 V. An upper limit of 4.5 V was defined since the hot spot mentioned above started burning at 5 V. Compared to glass substrates, flexible ones have poor heat dissipation due to the low thermal diffusivity of plastics. In Figure 4f, we compared the luminance of 8 mm^2 devices with 4 cm^2 devices in the same voltage range. The 8 mm^2 devices show an exponential increase of the luminance compared with an almost linear increase of the luminance in 4 cm^2 devices. This behavior must be expected given the higher current density driven through pixels with a smaller area, provided that the other characteristics (electrode pattern, structure, etc) of the QLEDs are similar. Further studies are guaranteed to simultaneously increase the luminance and reduce the Joule heat generation over the same voltage range. This can be achieved by improving the charge injection

balance to increase the EQE, increasing the conductivity of the charge transport layers for faster charge extraction, and reducing the electrodes sheet resistance by changing the materials or the pattern design. For instance, by changing the pattern design and size of the ITO-PEN substrates, we have observed that the luminance of 16 mm^2 pixels is 3.8x the luminance of the 8 mm^2 devices described in this work at the same voltage (3 V). Accordingly, the distance between the electrical contacts and the emissive area was reduced, and the ratio emissive area / ITO electrode area was increased (always < 1).

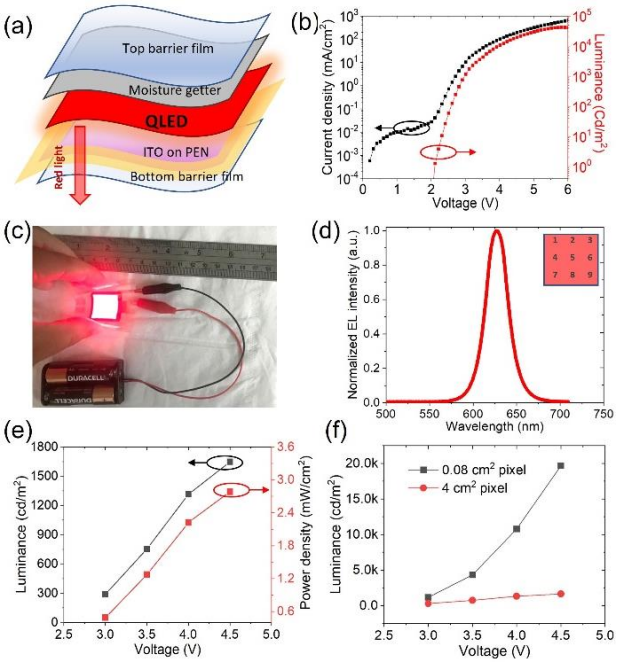

Fig 4. a) Structure of the encapsulated flexible QLEDs. b) J-L-V curves of the flexible QLEDs with 8 mm^2 pixels. c) Flexible QLED with emitting area of 4 cm^2 driven at 3 V in air. d) EL spectrum of the flexible QLEDs. Inset: location of points measured on the emissive area (L @ 3 V). e) L-V and OPD-V curves of the QLED with emissive area of 4 cm^2. f) L-V curves of the QLEDs with 8 mm^2 and 4 cm^2 pixels.

4 CONCLUSIONS

We have carried out on-glass QLED-based in vitro studies in PDT and PBM showing all satisfactory results. Our PBM in vitro studies for cell metabolism and migration promotion demonstrated the potential of QLED based PBM treatments for impaired wound healing and suggested further optimization at longer wavelengths. The PDT in vitro tests for the destruction of cancer cells also showed promising results, with efficacies of QLED-based PDT superior to those of in vitro PDT using commercial LEDs. In addition, the aPDT in vitro test demonstrated the high efficacy and simplicity of QLED-based aPDT for infected wound treatment and promises inactivation of pathogens without the risk of inducing resistance.

A controlled spectral overlapping for targeted phototherapy of different disorders or conditions was demonstrated by simply tuning the conditions of the QD synthesis and considering the emission red-shift observed in the EL of QLEDs. Additionally, our QLEDs fulfill other current needs, i.e., low-cost fabrication due to solution processing of functional layers, ergonomic factor due to reasonable flexibility and lightweight, homogeneous irradiation, and large emitting area (8 mm^2 - 4 cm^2) to target large lesions. Previously reported devices with 8 mm^2 pixels showed a record brightness among flexible red QLEDs. Here we also presented QLEDs with emitting area of 4 cm^2, narrow bandwidth emission, and low turn-on voltage (1.6 V). Although the emission area was increased 50x with respect to 8 mm^2 pixels, the maximum power density for safe operation (2.8 mW/cm^2 at 4.5 V) was still sufficient for low irradiation phototherapy such as metronomic photodynamic therapy (mPDT), and the power can be supplied from a small battery pack. While there are remaining challenges related to improving the encapsulation method, thermal management and scaling up of the devices, the results presented here represent an important step and guarantee further studies towards flexible QLEDs as suitable photomedical light sources.

REFERENCES

[1] Lanzafame RJ, Stadler I, Dong Y, Chen H, Wu S-T, He J. Preliminary studies of a novel red-emitting quantum dot LED source for photobiomodulation applications. *Laser Surg Med*, 49, pp. 57-8 2017.

[2] Chen H, He J, Lanzafame R, Stadler I, Hamidi HE, Liu H, et al. Quantum dot light emitting devices for photomedical applications. *J Soc Inf Display*, 25(3), pp. 177-84 2017.

[3] Lanzafame RJ, Stadler I, Dong Y, Chen H, He J, Blackman J, et al. Preliminary studies of a novel red-emitting quantum dot LED source for photobiomodulation for In Vitro model of the wound healing. *Laser Surg Med*, 50(4), pp. 359-60 2018.

[4] Chen H, Yeh T-H, He J, Zhang C, Abbel R, Hamblin MR, et al. Flexible quantum dot light-emitting devices for targeted photomedical applications. *J Soc Inf Display*, 26(5), pp. 296-303 2018.

[5] Triana MA, Wu S, Dong Y. P - 105: Bright, Large Pixel, Flexible Quantum - Dot Light - Emitting Diodes for Photomedicine. SID Int Symp Dig Tec, 51, pp. 1748-51 2020.

[6] Triana MA, Restrepo AA, Lanzafame RJ, Palomaki P, Dong Y. Quantum dot light-emitting diodes as light sources in photomedicine: photodynamic therapy and photobiomodulation. *JPhys Materials*. 3(3), pp. 032002 2020.